Catalysis Communications 10 (2009) 1925–1930

Contents lists available at ScienceDirect

Catalysis Communications

journal homepage: www.elsevier.com/locate/catcom

SAPO-34 supported Pt–Sn-based novel catalyst for propane dehydrogenation to propylene

Zeeshan Nawaz, Xiaoping Tang, Qiang Zhang, Dezheng Wang, Wei Fei *

Beijing Key Laboratory of Green Chemical Reaction Engineering and Technology, Tsinghua University, Beijing 100084, PR China

ARTICLE INFO

Article history:
Received 20 May 2009
Received in revised form 1 July 2009
Accepted 3 July 2009
Available online 3 August 2009

Keywords:
Pt–Sn-based catalyst
SAPO-34 support
Selective propane dehydrogenation
Propylene

ABSTRACT

The Pt–Sn-based catalyst was intensified using SAPO-34 as support for direct propane dehydrogenation to propylene. The catalyst was prepared by sequential impregnation method and characterized by XRF, BET, XRD, NH_3-IR, NH_3-TPD, H_2-TPR, HR-TEM and O_2-pulse coke analysis. NH_3-TPD, IR spectra and XRD results suggested that the doping of metals on SAPO-34 did not affect its acidic strength and structural topology of support, respectively. Propylene selectivity of 94% and total olefins selectivity greater than 97% was achieved using Pt–Sn/SAPO-34. The results were compared with Pt–Sn/ZSM-5 under identical conditions. The possible reasons for improvement were the larger surface area, shape selectivity and particular by suitable acidity of SAPO-34.

1. Introduction

Propylene is an indispensable raw material for numerous products and direct propane dehydrogenation process is believed to have good potential with minimum investment as a propylene production booster, in order to meet growing market demand [1,2]. On the other hand, propane is a low cost raw material and easily available. However, the reaction of direct propane dehydrogenation is highly endothermic ($\Delta H_R^{298\ K}$ = 125 kJ/mol of extracted hydrogen) requiring a relatively high temperature and lower pressure. Therefore a suitable catalyst of superior stereo-chemistry control is needed.

Pt–Sn-based catalysts supported on amorphous supports or zeolites, for propane dehydrogenation have been discussed in many studies [2–11]. The selection of Sn as a promoter has been explained in terms of geometric and/or electronic effects [12]. In the geometric effect, Sn decreases the size of platinum ensembles, which reduces hydrogenolysis and coking reactions. Sn also modifies the electronic density of Pt, either by positive charge transfer from the Sn^{n+} species or the different electronic structures in Pt–Sn alloys [13]. Therefore we can infer that the dehydrogenation performance of Pt–Sn-based catalysts depends on the interactions between the Pt and Sn species as well as the support. The deactivation of Pt-based catalyst during propane dehydrogenation is fatal, and mainly due to the aggregation of Pt particles and carbon deposition [13,14]. The Sn as a promoter helps in dispersing Pt metal and largely suppresses coke forming reactions, therefore significantly improves catalytic performance [10,14]. However, the mechanistic understanding is still controversial and the reaction results were not conclusive, especially on stability and selectivity.

Much focus has been given to Pt–Sn-based catalysts supported on Al_2O_3 for propane dehydrogenation [4,6]. But the lifetime of these catalysts is too short. Therefore, there is a growing interest in developing zeolite supported catalysts, e.g. Pt–Sn/ZSM-5 zeolite for propane dehydrogenation, because of longer activation times and higher conversions [2,10]. Many studies have improved the performance of Pt–Sn/ZSM-5 catalysts by adding a more metallic promoter (particularly from alkali or alkaline earth metals) like Na, Fe, Zn, etc. [2,5,15,16] and by increasing the Si/Al ratio of the ZSM-5 support [2]. However, ZSM-5 supported catalysts were detrimentally affected by frequent regeneration with steam [17] and have lower propylene selectivity [2]. ZSM-5 supported catalysts can further take part in cracking and their large pore size fails to create shape selectivity effect for propylene. Moreover comparing the effects of supports and additional promoters, it was observed that the performance of propane dehydrogenation reaction significantly dependent on support. In particular it was noted that the control of intermediates products to desired product over the bifunctional catalyst was significantly support dependent. These motivations provide the room for SAPO-34 zeolite as support of Pt–Sn-based catalyst.

In this work, the novel weak acidic support SAPO-34 (almost inert to dehydrogenation), with good shape selective opportunities

* Corresponding author. Tel.: +86 10 62784654; fax: +86 10 62772051.
E-mail address: wf-dce@tsinghua.edu.cn (W. Fei).

1566-7367/$ - see front matter © 2009 Elsevier B.V. All rights reserved.
doi:10.1016/j.catcom.2009.07.008

was experimentally investigated in order to improve propylene selectivity from direct propane dehydrogenation. The silicoaluminophosphate zeolite SAPO-34 is a microporous sieve with a chabasite-like structure (structural code CHA), has an extremely good shape selective effect for propylene [18–20]. Their Bronsted acid sites are responsible for their activities and based on two distinct hydroxyls (OH-bridges to Al and Si) on the structural framework. The structure, acidity and catalytic properties of SAPO-34 depend on the number and distribution of Si in the framework [21,22]. Its Si based acid sites make it resistant to hydrothermal treatment and gives superiority over ZSM-5, where dealumination occur frequently [15,16]. These observations suggest that the weak acidic support SAPO-34, which can sophisticatedly control the stereo-chemistry and gives shape selectivity effect for propylene in addition to being a bi-functional catalyst, Pt–Sn/SAPO-34.

A SAPO-34 supported novel Pt–Sn-based catalyst was proposed for direct propane dehydrogenation to propylene. However, no study to date has been focused on Pt–Sn-based catalyst's intensification using SAPO-34 as support that demonstrates superior propylene yield and selectivity. Therefore this study has aimed to examine the performances of Pt–Sn/SAPO-34 catalyst in a microreactor and its detailed characterization in order to justify SAPO-34 superiority as a support. The reaction mechanism for selective propane dehydrogenation to propylene over Pt–Sn/SAPO-34 was also characterized. In contrast, Pt–Sn/ZSM-5 catalyst results were compared under identical conditions to provide comprehensive information in understanding roles of the catalyst support.

2. Experimental

2.1. Catalyst preparation

The SAPO-34 catalyst was prepared by mixing Al_2O_3:P_2O_5:SiO_2:TEA:H_2O in the molar ratio of 1:1:0.5:2:100. This was stirred to make a uniform solution and then left for aging for 24 h at room temperature. The solution was put in an autoclave at 200 °C under autogenous pressure. After 24 h the product was filtered, dried and finally calcined at 550 °C for 4 h (BET surface area 441 m^2/g). The monometallic catalyst was prepared at 65 °C by co-impregnation of the above prepared SAPO-34 powder with a 0.03 M H_2PtCl_6 aqueous solution. After the impregnation, the catalyst was dried at 110 °C, and finally calcined at 500 °C for 4 h.

The bimetallic Pt–Sn-based SAPO-34 zeolite supported catalyst was prepared by sequential impregnation method, with calcined SAPO-34 powder. The SAPO-34 zeolite was first impregnated with 0.16 M $SnCl_2.2H_2O$ aqueous solution at 80 °C, to ensure 1 wt.% Sn component in the catalyst. After the impregnation, the catalyst was dried at 110 °C for 3 h and finally calcined at 500 °C in a muffle furnace for 4 h. In a second step, the prepared Sn/SAPO-34 catalyst was co-impregnated again with 0.03 M H_2PtCl_6 aqueous solution at 65 °C to give a 0.5 wt.% Pt component in the final the catalyst. Afterwards the same procedure was repeated, and the prepared samples were dried at 110 °C for 3 h and calcined at 500 °C for 4 h. Pt–Sn-based ZSM-5 (Si/Al ratio = 140) supported catalysts were prepared similarly. The prepared catalyst samples were crushed and used in pure form without pelletization.

2.2. Catalyst characterization

2.2.1. X-ray diffraction

The X-ray diffraction (XRD) patterns of powdered catalysts were obtained on a powder X-ray diffractometer (Rigaku-2500) with a copper anode tube. The X-ray tube was operated at 40 kV and 40 mA. The Kα radiation was selected with a monochromator. The spectra were scanned at a rate of 5°/min, from 5° to 45° (an angular range 2θ).

2.2.2. Metallic content measurement

The metallic contents were obtained by X-ray fluorescence (XRF) measurements on a Shimadzu XRF 1700 fluorimeter.

2.2.3. BET surface area measurement

The BET surface area was measured using N_2 adsorption/desorption isotherms determined at liquid nitrogen temperature on an automatic analyzer (Autosrb-1-C). The samples were out gassed for 1 h under vacuum at 300 °C prior to adsorption. The specific total surface areas of prepared samples were calculated using the BET equation.

2.2.4. IR spectroscopy

The IR spectra of adsorbed ammonia were recorded using a NEXUS apparatus (Nicolet, USA). The samples were dried, pressed into thin wafers and placed in a Pyrex glass cell equipped with CaF_2 window. Then the samples were degassed at 400 °C for 30 min and cooled to room temperature. Afterwards, ammonia was passed over the sample for 30 min and their adsorption spectra were recorded, after ammonia desorption at 100 °C.

2.2.5. Temperature-programmed desorption of ammonia

The acid properties of Pt and Pt–Sn doped catalysts were determined by NH_3-TPD on an Autochem-II 2920 analyzer. About 0.2 g of each catalyst sample was placed into a U-type quartz reactor. The samples were treated by flowing dry argon (99.99%) at 500 °C for 1 h prior to adsorption of ammonia. Then, samples were saturated with ammonia at room temperature. Before the run, the baseline was stabilized in argon (30 ml/min) at the same temperature. Afterwards, the temperature was kept at 100 °C for 0.5 h to desorb physically adsorbed ammonia. Subsequently, the temperature was raised to 600 °C at a heating rate of 10 °C/min. The NH_3 desorption profile was observed using a thermal conductivity detector.

2.2.6. Temperature-programmed reduction by hydrogen

Temperature-programmed reduction experiments were carried out on a conventional setup (same apparatus as used for NH_3-TPD) consisting of a programmable temperature furnace attached to Autochem-II 2920 analyzer. Samples (0.2 g) were loaded into the quartz reactor. Prior to TPR analysis, the samples were dried by flowing N_2 at 500 °C for 1 h (30 ml/min). The reactor was heated gradually from room temperature to 800 °C (10 °C/min). A 5% (v/v) H_2/N_2 mixture was used as reducing gas at the flow rate 30 ml/min. Hydrogen consumption as a function of reduction temperature was continuously monitored by a TCD cell and recorded.

2.2.7. O_2-pulse coke analysis

The amount of coke formed on catalysts during the dehydrogenation reaction was determined by O_2-pulse experiments, using a gas chromatograph flow system equipped with a TCD. The experiments were carried out at 750 °C by injecting pulses of pure oxygen (99.99%) onto the used catalysts (0.02 g). The CO_2 formed was continuously measured by a TCD detector and recorded. The pulses of pure O_2 were continued until deposited coke was fully removed. The amount of coke deposited on the catalysts was calculated from the amount of CO_2 generated.

2.2.8. TEM analysis

The Pt metal dispersion on support was verified using a JEM 2010 high-resolution transmission electron microscope (TEM) equipped with energy dispersive spectroscopy, operated at 120.0 kV before and after the reaction, for hydrothermally treated samples. The sample for TEM observation was prepared using a common sonication method, while thick samples were dispersed in ethanol.

2.3. Catalytic activity evaluation

The prepared catalyst samples were tested for propane dehydrogenation in a continuous flow microreactor at atmospheric pressure. 99.5% pure propane was used as feed in the current experimental investigation (provided by Zhong Ke Hui Jie HJAT, Beijing, China). A measured amount of catalyst samples was loaded into the reactor to maintain the desired WHSV (i.e. 5.6 h^{-1}). Prior to each reaction test, the catalysts was dechlorinated at 500 °C for 4 h with steam and then reduced under flowing H_2 with a molar flow rate of 8 ml/min at 500 °C, for 10 h. The reaction mixture composed of H_2 and C_3H_8 in a molar ratio 0.25 was charged into the microreactor. The product distribution was analyzed by an online gas chromatography (50-m PLOT Al_2O_3 capillary column) equipped with a FID detector. The conversions, selectivity's and yields presented in this paper are calculated in weight percentages.

3. Results and discussion

3.1. Effect of the novel support SAPO-34 on Pt–Sn-based catalyst performance

The superiority of novel support SAPO-34 performance was experimentally verified, and it was observed that Pt–Sn/SAPO-34 catalyst controls the stereo-chemistry of propane dehydrogenation reaction in well defined manner. The performances of Pt–Sn-based catalysts for selective propane dehydrogenation using both SAPO-34 and ZSM-5 zeolites as the carrier were tested under identical conditions, and results are shown in Fig. 1. The experimental results showed that SAPO-34 was almost inert for dehydrogenation as the conversion was less than 3.5%. The Pt–Sn/ZSM-5 showed a higher dehydrogenation rate but lower propylene selectivity i.e. about 40 wt.% [2]. The higher conversion of ZSM-5 catalyst is due to its contribution towards cracking. However, the Pt–Sn/SAPO-34 performance was far better, with above 94 wt.% propylene selectivity and with higher yield.

The different effect of SAPO-34 and ZSM-5 as the support of Pt–Sn-based catalysts on the propane dehydrogenation reaction can be shown using the olefins performance envelop (OPE). This is shown in Fig. 2. It can be seen that the Pt–Sn/SAPO-34 catalyst showed very high propylene and total olefins yields in comparison with Pt–Sn/ZSM-5. This suggested that shape selectivity may play a vital role. The coke formed over Pt–Sn-based ZSM-5 and SAPO-34 supported catalysts (of similar contents), under identical operating conditions (8 h operation) were 0.7 and 0.4 wt.% respectively. Moreover the surface area of SAPO-34 supported catalyst is larger than ZSM-5 supported catalyst. Propane conversion and propylene selectivity of ZSM-5 and SAPO-34 supported catalysts were compared in Table 1 under identical condition. It was observed that ZSM-5 itself is active for dehydrogenation due to higher surface acidity while SAPO-34 shows negligible conversion. Therefore later we stated it as inert towards dehydrogenation. The selectivity's comparison clearly demonstrates Pt–Sn/SAPO-34 superiority. The detailed product distribution over Pt–Sn/SAPO-34 was shown in Table 2.

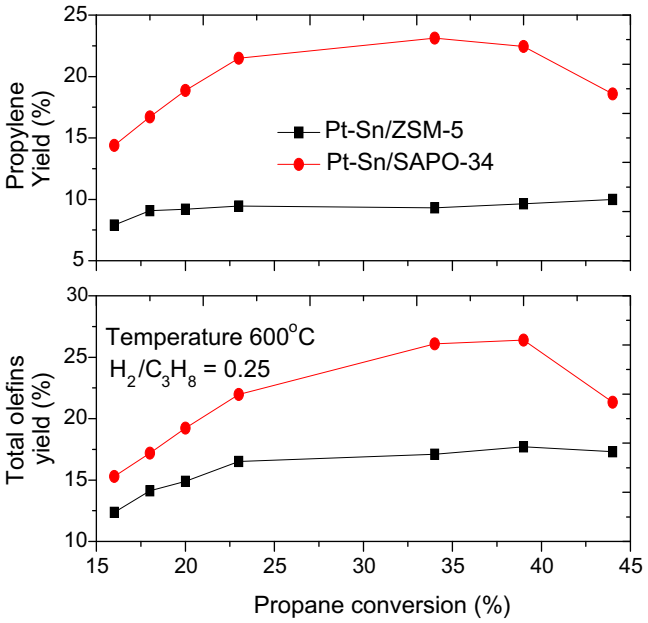

Fig. 2. OPE – Propylene and total olefin yields as a function of propane conversion.

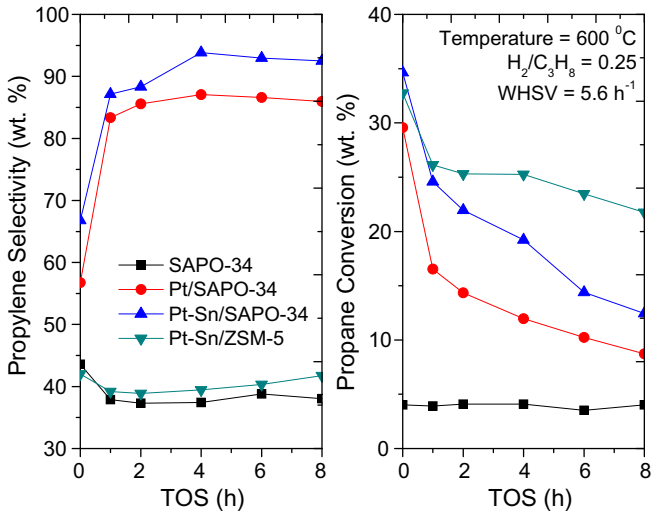

Fig. 1. Influence of different zeolite supports on propane dehydrogenation.

Previously, attempts have been given to improve the catalyst performance by varying metallic contents [5,15]. These tactics gave some achievements in obtaining desired results, but their side problems also brought about serious challenges. The most serious problem was dealumination of the support during regeneration with steam as ZSM-5 has an Al based structure. And the addition of promoter like Na, Fe, Zn, K, etc. can also increase the reaction with the steam, and Zn, Mn, etc. can lead the reaction towards aromatization. These built-in defects can be eliminated by using the inherently robust novel support SAPO-34, whose structure is Si based and resistant to hydrothermal treatment [23,24].

Higher propylene and total olefin yields were obtained at 40 wt.% conversion for both catalysts (see Fig. 2). The highest dehydrogenation activity and propylene selectivity was observed using Pt–Sn/SAPO-34. Pt–Sn/ZSM-5 exhibited the poorer propylene selectivity; most likely due to its stronger Bronsted acid sites which favor cracking too, and also due to that the larger pore size did not give shape selectivity. In contrast, SAPO-34 can control the stereo-chemistry of the overall reaction efficiently and can give shape selectivity effect for propylene.

It was interesting to find that the reaction stability and activity of Pt(0.5 wt.%)–Sn(1 wt.%)/SAPO-34 was superior to that of Pt(0.5 wt.%)–Sn(1 wt.%)/ZSM-5. The deactivation trends and coke formed at different catalysts are shown in Table 3. The amount of coke formed over the SAPO-34 supported catalysts was about 30% less than ZSM-5 supported catalysts, after 8 h reaction. Nevertheless, deactivation and/or activity loss of the catalyst is not only

Table 1
Comparison of ZSM-5 and SAPO-34 supported catalysts performance at time-on-stream 1 h, 600 °C and 5.6 h^{-1} WHSV.

Catalyst	Conversion (%)	Propene selectivity (%)	Catalyst	Conversion (%)	Propene selectivity (%)
ZSM-5	28.73	20.76	SAPO-34	3.42	38.74
Pt/ZSM-5	27.11	35.29	Pt/SAPO-34	17.62	84.51
Pt–Sn/ZSM-5	27.56	39.83	Pt–Sn/SAPO-34	25.13	88.39

Table 2
Detailed product distribution over Pt–Sn/SAPO-34 at time-on-stream 2 h, 600 °C and 5.6 h^{-1} WHSV.

Product	Selectivity (%)	Yield (%)
Methane	1.17	0.26
Ethane	1.06	0.23
Ethylene	1.81	0.44
Propylene	88.39	22.36
Butane	4.89	1.29
Butene	2.68	0.67

Table 3
Deactivation as a function of different Pt–Sn catalysts. The deactivation parameter was defined as $D_r = [(X_0 - X_f)/X_0 \times 100]$; where, X_0 is the initial conversion at 1 min, X_f is the final conversion and S_f is the final selectivity at 8 h. The reaction temperature was 600 °C.

Catalysts	X_0	X_f	D_r	[a]Coke	S_f
SAPO-34	3.71	3.69	0.01	0.07	38.2
Pt(0.5 wt.%)/SAPO-34	29.9	10.6	19.3	0.37	84.1
Pt(0.5 wt.%)–Sn(1 wt.%)/SAPO-34	34.8	14.1	20.7	0.42	94.9
Pt(0.5 wt.%)–Sn(1 wt.%)/ZSM-5	33.3	22.7	10.6	0.66	43.5

[a] O_2-pulse coke analysis.

due to coke deposition. Moreover it was observed that the amount of coke formed was related to catalysts activity (Table 4).

3.2. Characterization of Pt–Sn/SAPO-34 catalyst

3.2.1. X-ray diffraction

The X-ray diffraction patterns of the SAPO-34 supported catalysts with different metallic contents were shown in Fig. 3. After sequential impregnation of metallic solutions, the original structure of the SAPO-34 zeolite support was still the same. This indicated that the metallic doping during catalyst preparation did not destroy the structural topology of SAPO-34. The average diameter of Pt metal particles ranges from 1.4 to 2.5 nm [17,25], is too large to enter into the SAPO-34 channels. Therefore, we can assume that the platinum particles were only located on the external surface of the zeolite. Furthermore, no new PtO_2 species were found in Fig. 3, suggesting that the platinum species were well dispersed/interacted on the external surface of the catalyst [26]. Interestingly, the intensities of the corresponding peaks at angle $2\theta = 8°–10°$ decreased much with Sn loading, indicating that the addition of Sn affected the crystallinity of the SAPO-34 zeolite. Meanwhile no peak shift was observed.

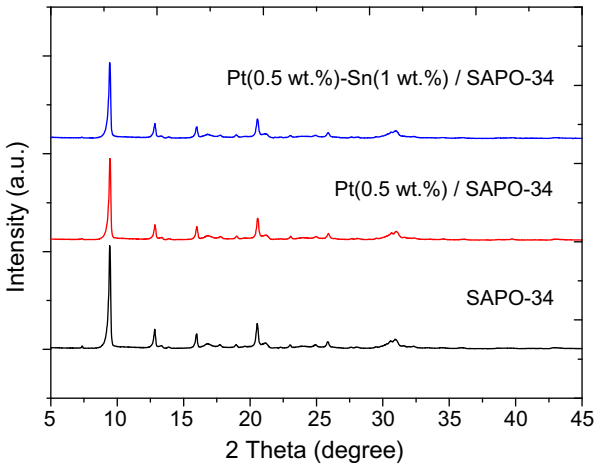

Fig. 3. XRD patterns of the SAPO-34 supported catalysts with different metallic combinations.

3.2.2. Basic catalyst characterizations

The compositions of the different catalysts were obtained from XRF analysis, and shown in Table 2. Therefore it was confirmed that the metallic contents were successfully loaded on the support by sequential impregnation method. The surface area tends to decreased with metallic loadings as indicated by BET results in Table 2. The surface area of the Pt(0.5 wt.%)–Sn(1 wt.%)/SAPO-34 catalyst was found greater than Pt(0.5 wt.%)–Sn(1 wt.%)/ZSM-5. The metal doping most likely blocked some of the pores of the zeolite support, thereby causing loss of surface area. It is probable that most of the Sn were located on the external surface and in the vicinity of pore mouths of the zeolite.

3.2.3. IR spectroscopy analysis

Ammonia adsorption IR spectroscopy is a useful technique for measuring and characterizing the acid sites of SAPO-34 and SAPO-34 supported catalysts. Fig. 4 shows the ammonia adsorption behavior of different samples evaluated at 100 °C. It can be seen that SAPO-34 has Lewis and Brönsted acid sites from the ammonia absorption bands at 1610–1630 cm^{-1} and 1420–1460 cm^{-1}, respectively. Accordingly, it was found that SAPO-34 and SAPO-34 supported catalysts have both weak Bronsted and Lewis acid sites. The intensities of the corresponding bands associated with chemisorbed ammonia were decreased, when desorption takes place at 100 °C, in contrast to original SAPO-34 zeolite. The

Table 4
Basic catalysts characteristics.

Catalysts	[a]Pt content (% w/w)	[a]Sn content (% w/w)	[b]S_{BET} (m^2/g)
SAPO-34	–	–	441
Pt(0.5 wt.%)/SAPO-34	0.50	–	424
Pt(0.5 wt.%)–Sn(1 wt.%)/SAPO-34	0.32	0.87	419
Pt(0.5 wt.%)–Sn(1 wt.%)/ZSM-5	0.49	0.84	396

[a] Results from XRF analysis.
[b] Calculated from N_2 physi-sorption using BET equation.

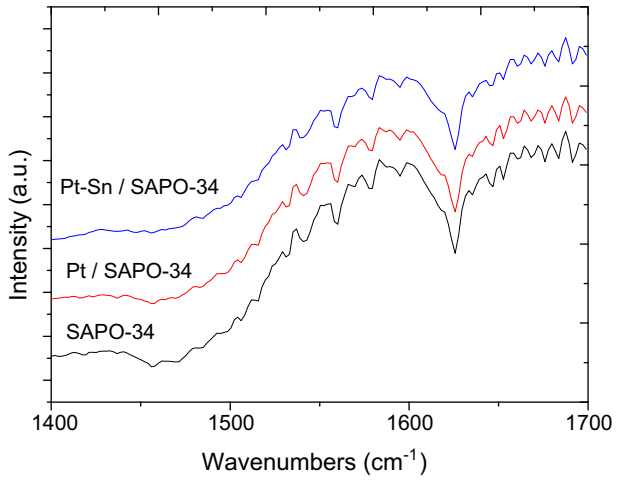

Fig. 4. IR spectra of ammonia adsorbed on the different catalysts and desorbed at 100 °C.

intensities of the corresponding peaks decreased after loading with Pt and Sn. One possible explanation for this behavior was the location of Pt atoms on Bronsted acid sites, thus consuming some acid sites [27]. At the same time, the Sn promoter is believed to reduce the Lewis acid sites on the catalyst [28]. This can leads to a more clear division of catalyst functionality and enhance propylene selectivity.

3.2.4. NH_3-temperature-programmed desorption analysis

The acidic profiles of prepared catalysts were examined by NH_3-TPD analysis. Their profiles were shown in Fig. 5. Two ammonia desorption peaks were observed. The first desorption peak between 200 and 230 °C was assigned to the weak acid sites. The second peak between 400 and 430 °C corresponds to the strong acid sites. The decrease in strong acid sites was expected because the Pt consumed some of the Bronsted acid sites on SAPO-34. Also small shifts in peak positions were noted. In general, no substantial decrease in the acidity of the system was observed after the metallic doping. And this weak acidity was valuable to control intermediates selectively.

3.2.5. Temperature-programmed reduction with hydrogen

The influences of the metals doping on the reduction properties of the SAPO-34 supported catalysts were measured by H_2-TPR. The TPR profiles of all samples were shown in Fig. 6. There was no reduction peak appears for the SAPO-34 zeolite, while the Pt/SAPO-34 catalyst shows sharp reduction peak between 450 and 600 °C. The reduction peaks at the higher temperature indicated that the Pt was strongly interaction with the SAPO-34. The H_2 reduction results of Pt–Sn/SAPO-34 displayed wide reduction peak between 360 and 540 °C that confirmed the joint reduction and valuable interaction between Pt and Sn on the SAPO-34. The similar discussion was reported in previous studies [10,29]. Moreover, it has been widely reported in the literature that the presence of Sn can strongly influenced the oxidation and reduction properties of Pt [10,30,31]. The formation of the Pt–Sn alloy results permanent deactivation [10]. This situation mostly occurs when the Pt and Sn concentration was in excess, in comparison with the acid sites providing by support. That form layer over the support and deceases catalytic activity.

3.2.6. TEM analysis

The TEM image of Pt–Sn/SAPO-34 catalyst was shown in Fig. 7. The agglomerations of Pt particles were not observed; moreover the Pt particles were found to be well dispersed over the surface of support. The presence of Pt on the surface was further verified by EDS attached to HR-TEM. These results supports above discussion.

3.3. Reaction mechanism

Direct propane dehydrogenation can proceed by three routes, (a) protolytic dehydrogenation (together with cracking) on Brønsted acid sites [32], (b) dehydrogenation on species affiliated with extra aluminum moieties of the support framework [33], and (c) dehydrogenation on reduced metallic sites. Thomas et al. have extensively studied the mechanism of light alkane conversion over H-ZSM-5 and showed that carbonium ions were the intermediates for all primary reactions on acid sites [32]. However, when SAPO-34 is used, carbonium ion formation from propane is difficult due to the low Bronsted acidity (see IR and TPD results). Therefore it can be concluded that the acid sites provided by SAPO-34 would be insufficiently for light alkane cracking and dehydrogenation. These results were further verified from experimental results as shown in Fig. 1 and Table 1.

Therefore on a Pt-based SAPO-34 supported catalyst, propane dehydrogenation proceeds by hydrogen abstraction on metallic sites in which a propoxy species ($Z–O–C_3H_7$) was formed. For the dehydrogenation of propane on Pt–Sn/SAPO-34, only one hydrogen (attached to a β-carbon) is available for attack with the reduced

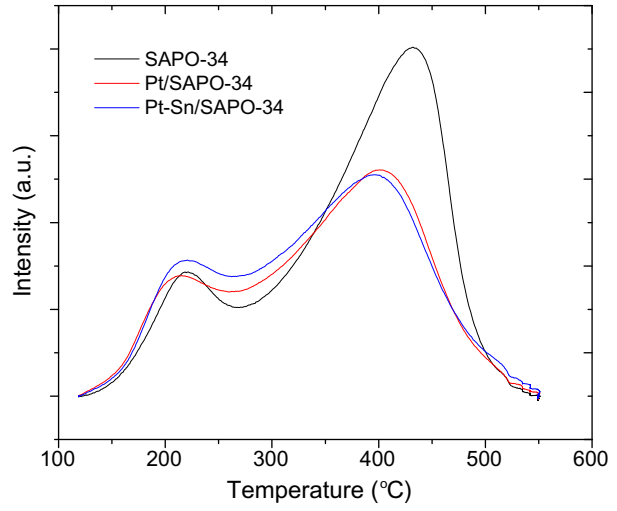

Fig. 5. NH_3-TPD profile of SAPO-34 and SAPO-34 supported catalysts.

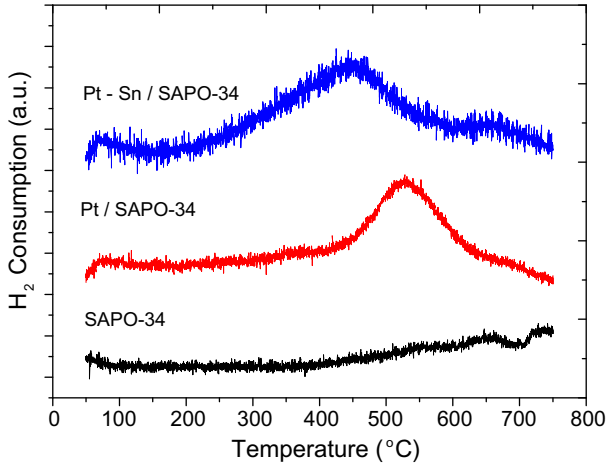

Fig. 6. H_2-TPR profiles of the SAPO-34 supported catalysts.

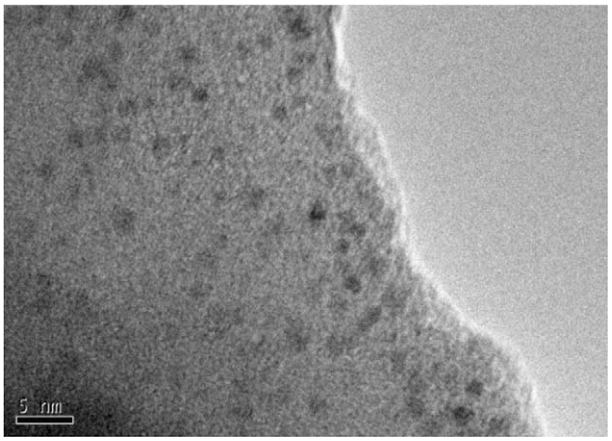

Fig. 7. HR-TEM image of Pt–Sn/SAPO-34.

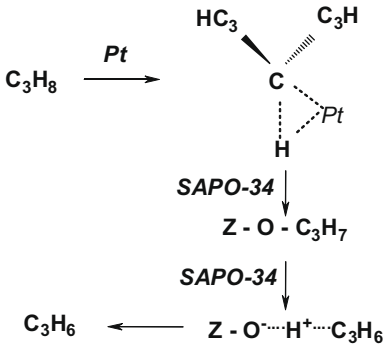

Scheme 1. Propane dehydrogenation mechanism over a Pt-based SAPO-34 supported catalyst.

metal. A second proton abstraction from the propoxy species would be performed by framework oxygen atoms from the support. This could proceed through a transition state like ($Z–O^{-}\cdots H^{+}\cdots C_3H_6$). The SAPO-34 selectively performs this conversion better than other catalysts. The final step is propylene desorption. The intrinsic rates of dehydrogenation and olefin desorption were on the same order of magnitude [30]. The speculative reaction mechanism is shown in Scheme 1.

4. Conclusion

The superior catalytic performance of Pt–Sn/SAPO-34 was obtained due to weak acid sites that can convert propyl cation to propylene selectively. Moreover SAPO-34 was almost inert to dehydrogenation and cracking, and their shape selectivity effect which only allowed propylene to form. A Pt–Sn/SAPO-34 catalyst was prepared by sequential co-impregnation method. The metal doping and structure stability were confirmed by XRF and XRD, respectively. The SAPO-34 supported catalyst was much better than a ZSM-5 supported bimetallic catalyst. IR and TPD analysis suggested that both Lewis and Brönsted acid sites were exist on SAPO-34 supported catalysts and these were stable after metal incorporation. This suitable acidity selectively converts reaction intermediates to propylene. O_2-pulse analysis showed that SAPO-34 was better in accommodating coke and stabilize catalyst than ZSM-5. However, deactivation also occurred due to the loss in active metallic sites with time-on-stream. H_2-TPR results showed that the presence of Sn improved the reduction of Pt. In the propane dehydrogenation mechanism over Pt–Sn/SAPO-34, only one hydrogen attached to a β-carbon in propane was available for attack by Pt, to form the propoxy species ($Z–O–C_3H_7$). These propoxy species were selectivity converted to propylene over SAPO-34.

Acknowledgement

This research was financially supported by Natural Scientific Foundation of China (No. 20606020, No. 20736004, No. 20736007) and Higher Education Commission, Islamabad, Pakistan (No. 2007PK0013). The authors would like to be very thankful to FLOTU colleagues for their help in the experiments.

References

[1] D. Akporiaye, S.F. Jensen, U. Olsbye, F. Rohr, E. Rytter, M. Ronnekleiv, A.I. Spjelkavik, Ind. Eng. Chem. Res. 40 (2001) 4741–4748.
[2] N. Zeeshan, T. Xiaoping, W. Fei, Korean J. Chem. Eng. 6 (2009). pp. XXX–XXX.
[3] H. Lieske, J. Volter, J. Catal. 90 (1984) 96–105.
[4] G.D. Angel, A. Bonilla, Y. Pena, J. Navarrete, J.L.G. Fierro, D.R. Acosta, J. Catal. 219 (2003) 63–73.
[5] T. Waku, J.A. Biscardi, E. Iglesia, Chem. Commun. (2003) 1764–1772.
[6] F.B. Passos, M. Schmal, M.A. Vannice, J. Catal. 160 (1996) 106–117.
[7] P.L.D. Cola, R. Gläser, J. Weitkamp, Appl. Catal. A. Gen. 306 (2006) 85–97.
[8] M.S. Kumar, D. Chen, J.C. Walmsley, A. Holmen, Catal. Commun. 9 (2008) 747–750.
[9] S.M. Stagg, C.A. Quenrini, W.E. Alvarez, D.E. Resasco, J. Catal. 168 (1997) 75–94.
[10] Y. Zhang, Y. Zhou, A. Qiu, Y. Wang, Y. Xu, P. Wu, Catal. Commun. 7 (2006) 860–866.
[11] G. Aguilar-Rios, P. Salas, M.A. Valenzuela, H. Armendariz, J.A. Wang, J. Salmones, Catal. Lett. 60 (1999) 21–25.
[12] J. Llorca, N. Homs, J. Leon, J. Sales, J.L.G. Fierro, P. Ramirez, Appl. Catal. A. Gen. 189 (1999) 77–86.
[13] C. Kappenstein, M. Guierin, K. Liaziar, K. Matusek, Z. Paial, J. Chem. Faraday Trans. 94 (1998) 2463–2474.
[14] M.S. Kumar, D. Chen, A. Holmen, J.C. Walmsley, Catal. Today 142 (2009) 17–23.
[15] Y. Zhang, Y. Zhou, A. Qiu, Y. Wang, Y. Xu, P. Wu, Acta Phys.-Chim. Sin. 22 (2006) 672–678.
[16] Y. Zhang, Y. Zhou, H. Liu, Y. Wang, Y. Xu, P. Wu, Appl. Catal. A. Gen. 333 (2007) 202–210.
[17] Y. Zhang, Y. Zhou, K. Yang, Y. Li, Y. Wang, Y. Xu, P. Wu, Micropor. Mesopor. Mater. 96 (2006) 245–254.
[18] M.A. Anderson, B. Sulikowski, B.J. Barrie, J. Klinowski, J. Phys. Chem. 94 (1990) 2730–2734.
[19] Y. Xu, C.P. Grey, J.M. Thomas, A.K. Cheetham, Catal. Lett. 4 (1990) 251–260.
[20] J. Chen, P.A. Wright, J.M. Thomas, S. Natarajan, L. Marchese, S.M. Bradley, G. Sankar, C.R.A. Catlow, P.L. Gai-Boyes, R.P. Townsend, C.M. Lok, J. Phys. Chem. 98 (1994) 10216–10224.
[21] G. Sastre, D.W. Lewis, C. Richard, A. Catlow, J. Phys. Chem. B 101 (1997) 5249–5262.
[22] E. Dumitriu, A. Azzouz, V. Hulea, Micropor. Mesopor. Mater. 10 (1997) 1–8.
[23] L. Guangyu, T. Peng, L. Jinzhe, Z. Dazhi, Z. Fan, L. Zhongmin, Micropor. Mesopor. Mater. 111 (2008) 143–149.
[24] S. Wilson, P. Barger, Micropor. Mesopor. Mater. 29 (1999) 117–126.
[25] A.D. Lucas, J.L. Valverde, P. Sanchez, F. Dorado, M.J. Ramos, Appl. Catal. A. Gen. 282 (2005) 15–24.
[26] R. Rachapudi, P.S. Chintawar, H.L. Greene, J. Catal. 185 (1995) 58–72.
[27] P. Treesukol, K. Srisuk, J. Limtrakul, T.H. Truong, J. Phys. Chem. B 109 (2005) 11940–11945.
[28] O.A. Barias, A. Holmen, E.A. Blekkan, Catal. Today 24 (1995) 361–364.
[29] L.R.R. Araujo, M. Schmal, Appl. Catal. A. Gen. 235 (2002) 139–147.
[30] R.D. Cortright, J.A. Dumesic, Appl. Catal. A. Gen. 129 (1995) 101–115.
[31] T.F. Narbeshuber, A. Brait, K. Seshan, J.A. Lercher, J. Catal. 172 (1997) 127–136.
[32] S. Yanping, T.C. Brown, J. Catal. 194 (2000) 301–308.
[33] F.N. Thomas, V. Hannelore, A.L. Johannes, J. Catal. 157 (1995) 388–395.